Available online at www.sciencedirect.com
ScienceDirect
Ceramics International 37 (2011) 2625–2630
CERAMICS INTERNATIONAL
www.elsevier.com/locate/ceramint

On the structural and magnetic properties of La-substituted NiCuZn ferrites prepared using egg-white

M.A. Gabal [a,*], Abdullah M. Asiri [a,b], Y.M. AlAngari [a]

[a] Chemistry Department, Faculty of Science, King Abdul Aziz University, Jeddah, Saudi Arabia
[b] The Center of Excellence for Advanced Materials Research, King Abdul Aziz University, Jeddah, Saudi Arabia

Received 26 January 2011; received in revised form 30 March 2011; accepted 6 April 2011
Available online 13 April 2011

Abstract

$Ni_{0.50}Cu_{0.25}Zn_{0.25}La_xFe_{2-x}O_4$ ferrites (with $x = 0.00$–0.09) were prepared by a simple method using metal nitrates and freshly extracted egg white. The proper calcination temperature for ferrites formation was estimated using thermo-gravimetry technique (TG). The samples were characterized using X-ray diffraction (XRD), transmission electron microscopy (TEM) and infrared spectroscopy (FT-IR) measurements. XRD of the powders calcined at 550 °C for 2 h showed single-phase crystalline cubic ferrites with crystallite sizes in the range 17.2–21.6 nm. Both the lattice parameter and X-ray density are found to increase by the addition of rare earth ion. TEM image showed agglomerated nano-particles with irregular sizes and shapes. FT-IR spectra showed two absorption bands (ν_1 and ν_2) attributed to stretching vibration of tetrahedral and octahedral complex Fe^{3+}–O^{2-}, respectively. The shifting of the ν_2 band towards lower frequencies indicates the preference of lanthanum ions to occupy the octahedral sites. The effect of La-substitution on the magnetic properties was studied using vibrating sample magnetometry (VSM) and susceptibility measurements. The decrease in the saturation magnetization with increasing La content can be attributed to the decreasing of Fe^{3+}–Fe^{3+} interactions in the octahedral sites. Coercivity shows size dependent behavior due to the combination of surface effect and surface anisotropy. The obvious decrease in the Curie temperature (T_C) with increasing La content indicates that the highly paramagnetic character of La^{3+} ions decreases the ferromagnetic region at the expense of the paramagnetic one.

Keywords: La-substitution; NiCuZn ferrites; XRD; VSM; Susceptibility

1. Introduction

Spinel ferrites are used in the fabrication of multilayer chip inductors (MLCIs) as surface mount devices for miniaturized electronic products such as cellularphones, notebook computers, video camera recorders and floppy drives [1]. NiCuZn ferrites are a soft magnetic material with a completely inverse spinel structure [2]. They have been widely used in multilayer chip inductors and correlative inductive devices due to their low-sintering temperature, high electrical resistivity and excellent magnetic properties [3].

The nanostructured magnetic particles have different properties from the corresponding bulk material due to their reduced size and effect of magnetic interaction between particles [4]. Better magnetic properties of ferrite are essential for modern MLCIs to reduce the number of ferrite layer in the chip. The magnetic properties of the ferrite are highly sensitive to the amount of constituent metal oxides in their compositions [5]. Small amount of additives can also used to modify microstructure and hence magnetic properties. In this category, rare earth oxides are becoming promising additives to improve the magnetic properties of ferrites [4,6–8].

In many investigations [9–13], a modification in the structural, magnetic and electrical properties is obtained due to the addition of rare earth ions however, in some cases conflicting results are obtained. For these reasons, further studies on rare earth-substituted ferrites are needed. Therefore, purpose of our investigation is to study the effect of La^{3+} substitutions for Fe^{3+} on the structural and magnetic properties of NiCuZn ferrite.

* Corresponding author. Permanent address: Chemistry Department, Faculty of Science, Benha University, Benha, Egypt. Tel.: +966 557071572.
E-mail address: mgabalabdonada@yahoo.com (M.A. Gabal).

0272-8842/$36.00
doi:10.1016/j.ceramint.2011.04.007

Roy and Bera [8] synthesized $Ni_{0.25}Cu_{0.20}Zn_{0.55}La_xFe_{2-x}O_4$ ferrite (with $x = 0.00$–0.075) through nitrate–citrate auto-combustion method. Crystalline spinel ferrite phase was obtained in the as-burnt ferrite powder. Initial permeability, magnetic loss and AC resistivity of different compositions were measured. Saturation magnetization and hysteresis parameters were measured at room temperature. The best electromagnetic properties were obtained for the composition of $x = 0.025$, which would be better for more miniaturized multi layer chip inductor.

$Ni_{0.25}Cu_{0.2}Zn_{0.55}Sm_xFe_{2-x}O_4$ ferrite (with $x = 0.00$–0.075) was synthesized through the nitrate–citrate auto-combustion method. The effect of Sm substitution on phase composition, microstructure and relative density was studied. Permeability, magnetic loss and AC resistivity were also measured. The observed variations in electromagnetic properties have been explained.

In this article, we describe a simple and eco-friendly method to synthesize NiCuZn ferrite nanoparticles. La^{3+} ions were used as substitute for replacement of Fe^{3+} in ferrite to tailoring magnetic properties. The microstructural and magnetic properties of resulting nanoparticles were investigated by TG, XRD, FT-IR, TEM molar magnetic susceptibility and VSM measurements.

2. Experimental

$Ni_{0.50}Cu_{0.25}Zn_{0.25}La_xFe_{2-x}O_4$ ferrite (with $x = 0.00$–0.09) system was prepared by a simple method using metal nitrates and freshly extracted egg white in an aqueous medium [17]. The starting reagents used were $Ni(NO_3)_2{\cdot}6H_2O$, $Cu(NO_3)_2{\cdot}3H_2O$, $Zn(NO_3)_2{\cdot}6H_2O$, $La(NO_3)_3{\cdot}6H_2O$ and $Fe(NO_3)_3{\cdot}9H_2O$ and freshly extracted egg white. The detailed procedure was discussed previously [14,15].

The decomposition process was investigated by thermo-gravimetric analysis (TG) to determine the temperatures of the possible decomposition of precursors into ferrites. The analysis was performed using Perkin Elmer thermal analyzer with a heating rate of 5 °C/min in flowing air up to 600 °C. According to the TG results, all the precursors were calcined at 550 °C in a muffle furnace under static air for 2 h.

Structural changes of powder particles were studied by X-ray diffraction in a D8 Advanced diffractometer, Bruker AXS using filtered Cu Kα1 radiation (λ = 0.15406 nm) obtained in the 2θ range 20–70°.

Fourier transform infrared spectroscopy (FT-IR) was measured using a Jasco model FT-IR 310 spectrophotometer.

The morphology of the synthesized powders was examined using a transmission electron microscopy (TEM) JEOL 2010 operated at 100 kV.

The hysteresis behaviors were measured at room temperature by using the vibrating sample magnetometer (VSM) up to magnetic field of ±5 kOe.

The magnetic susceptibility was measured at different temperatures ranging from 300 to 850 K and at different magnetic field intensities of 1010, 1340, 1660 and 1990 Oe using Faraday's method. The temperature of the samples was measured using a T-type thermocouple with the junction near the sample to avoid any temperature gradient.

3. Results and discussion

3.1. Decomposition characterization

Thermal decomposition behavior of the egg-white precursors was investigated by using thermo-gravimetric (TG) analysis. They exhibited similar decomposition behavior. Here, we have discussed the thermal decomposition behavior of precursor powder with lanthanum content of 0.03 as a representative. TG curve (Fig. 1) shows a total weight loss of 72% when the sample was heated up to 600 °C in air. The weight loss of 19% occurred between 30 and 100 °C can be assigned to the hydrated water of the precursor. Successive weight losses observed between 100 and 400 °C could be attributed to the decomposition of the nitrate and organic contents of the precursor. It was observed that beyond 400 °C, there was no significant weight loss until 600 °C.

3.2. Structural characterization

In order to determine the optimum calcination condition to generate single phase La-substituted NiCuZn ferrite, room temperature powder XRD analysis of as-prepared egg-white precursors as well as precursors calcined at different temperatures was performed and the formation of crystalline phases due to calcination of different precursors was monitored.

Fig. 2 shows typical XRD pattern of the as-prepared precursor with La content of 0.03. The figure indicates complete amorphous behavior of the sample. Fig. 3 shows the X-ray patterns of the precursors calcined at 550 °C for 2 h. All

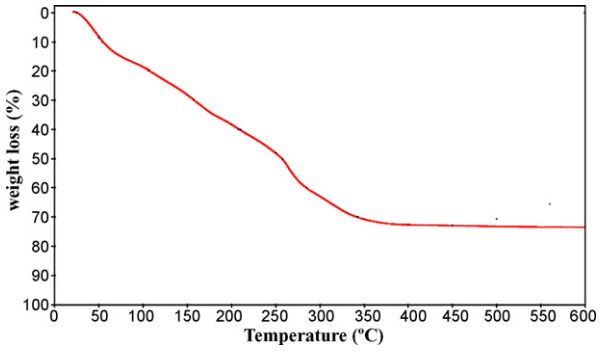

Fig. 1. TG curve in air of as-prepared egg-white precursor with La content of 0.03. Heating rate = 5 °C min^{-1}.

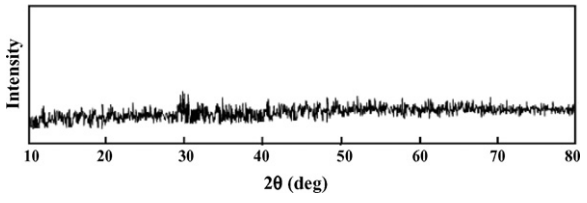

Fig. 2. XRD patterns of the as-prepared egg-white precursor with La content of 0.03.

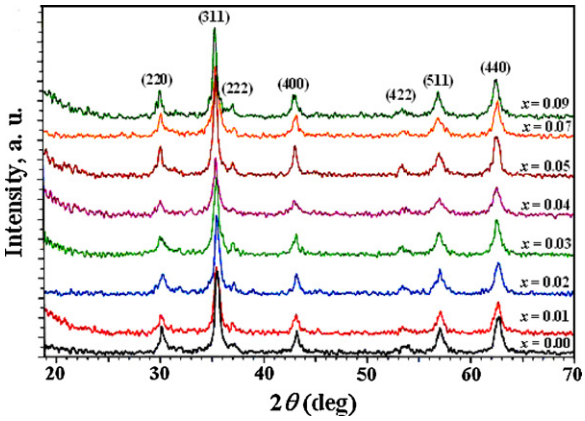

Fig. 3. Characteristic parts of XRD patterns of $Ni_{0.50}Cu_{0.25}Zn_{0.25}La_xFe_{2-x}O_4$ samples calcined at 550 °C for 2 h.

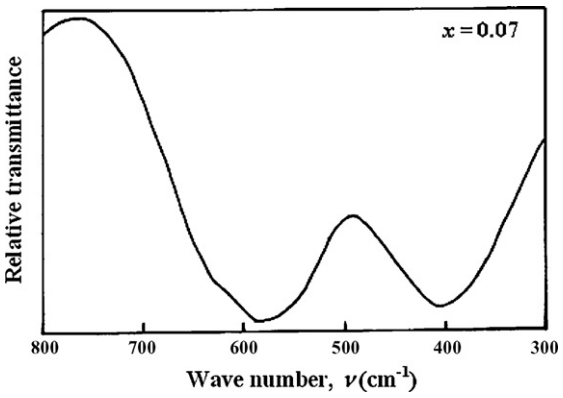

Fig. 4. TEM image of calcined sample with La content of 0.03.

the peaks are found to match well with those of single-phase cubic spinel ferrite (JCPDS card no. 08-0234). The most intense peaks in all the specimens are indexed as (2 2 0), (3 1 1), (2 2 2), (4 0 0), (4 2 2), (5 1 1) and (4 4 0). The background noise and broadness of the peaks are characteristic of particles with nanometer dimensions. This happens because in the nanosized particles there are insufficient diffraction centers that cause the line broadening [16].

It has been established that secondary phases are formed when La^{3+} is added to ferrites [8,10,11,17,18]. In the present work, no secondary phases were detected in XRD patterns of the calcined samples even at higher La contents. This unique behavior can be assigned to the effect of the utilized preparation method.

Lattice parameters and crystallite sizes of the sintered ferrite specimens, evaluated by XRD analysis, are represented in Table 1 along with their X-ray density. The lattice constant is observed to increase from 8.36 to 8.40 Å with increasing lanthanum content. This can be attributed to the higher ionic size of La^{3+} ions (1.016 Å) compared with that of Fe^{3+} ions (0.645 Å) [19]. The X-ray density gradually increases with increasing lanthanum substitution, indicating improved densification [4].

Transmission electron microscope was used to investigate the particle size of the ferrite nanoparticles, prepared from the egg-white precursor. The typical TEM image of ferrite nanopowder with $x = 0.03$ is shown in Fig. 4. The nanopowders were of average particle size of 19 nm, which agrees well with that estimated from the XRD data. They were irregular in size and shape. The particles tend to agglomerate because they experience a permanent magnetic moment proportional to their volume [20].

The analysis of FT-IR spectra can give information about structural transformation and can be considered as an important tool to get information about position of ions in the crystal. Fig. 5 shows typical FT-IR spectrum of the ferrite sample with lanthanum content of 0.03 in the range from 300 to 800 cm^{-1}. FT-IR spectral data of the investigated system are presented in Table 1. It is observed that, there are two main frequency bands, namely, high frequency band ν_1 (around 600 cm^{-1}) and low frequency band ν_2 (around 400 cm^{-1}). These two observed bands are corresponded to the intrinsic vibrations of tetrahedral and octahedral Fe^{3+}–O^{2-} complexes, respectively, and are the characteristics of all the ferrite composites [21]. The different band positions of ν_1 and ν_2 are expected because of different Fe^{3+}–O^{2-} bond lengths for tetrahedral and octahedral sites.

The shifting of the ν_2 band towards lower frequencies, with increasing lanthanum concentration, may be attributed to the increase in the unit cell dimensions as evidenced by the variation in the lattice constant. The increase in the unit cell dimensions due to the replacement of Fe^{3+} ions by larger ionic radius La^{3+} ions affects the Fe^{3+}–O^{2-} stretching vibrations and

Table 1
Lattice parameters, X-ray densities, average crystallite size, FT-IR spectral data and magnetic data of $Ni_{0.50}Cu_{0.25}Zn_{0.25}La_xFe_{2-x}O_4$ system.

Parameters	$x = 0.00$	$x = 0.01$	$x = 0.02$	$x = 0.03$	$x = 0.04$	$x = 0.05$	$x = 0.07$	$x = 0.09$
Lattice parameter (a), Å	8.3684	8.3710	8.3742	8.3788	8.3801	8.3870	8.3948	8.4093
X-ray density (D_x), g cm^{-3}	5.39	5.40	5.41	5.42	5.43	5.44	5.46	5.47
Average crystallite size (L), nm	18.0	17.5	17.2	19.1	20.8	21.6	19.2	19.8
Tetrahedral vibration (ν_1), cm^{-1}	583	586	584	584	585	585	584	586
Octahedral vibration (ν_2), cm^{-1}	408	405	404	403	399	398	396	392
Saturation magnetization (M_s), emu g^{-1}	40.5	39.6	39.3	38.3	38.0	39.1	36.8	37.4
Remenant magnetization (M_r), emu g^{-1}	3.6	6.3	6.6	7.9	8.3	9.5	6.9	8.9
Corecivity (H_c), emu g^{-1}	44.8	39.5	38.9	58.3	60.1	62	47.6	61.4
Magnetic moment (η_B), μ_B	1.72	1.69	1.68	1.65	1.64	1.69	1.60	1.64
Molar magn. suscept. (χ_M), emu g^{-1} mol^{-1}	7.3	6.1	9.4	9.6	6.2	9.0	7.1	1.1
Curie temperature (T_C), K	737	726	711	702	698	691	680	668

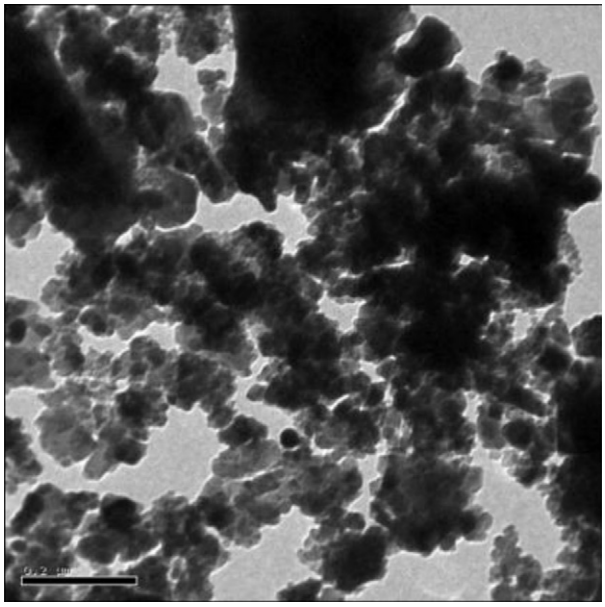

Fig. 5. FT-IR spectra of $Ni_{0.50}Cu_{0.25}Zn_{0.25}La_xFe_{2-x}O_4$ system calcined at 550 °C for 2 h.

this is a prominent cause of change in band positions. The very slight change in the frequency of ν_1 stretching band indicates the preference of lanthanum ions to occupy the octahedral sites.

3.3. Magnetic studies

3.3.1. Hysteresis behavior

The magnetic properties are the most important properties of ferrites depending on the processing conditions, microstructure, chemical composition and the type of the additives. Fig. 6 shows the magnetic hysteresis curve for $Ni_{0.50}Cu_{0.25}Zn_{0.25-}La_xFe_{2-x}O_4$ ferrites. The figure revealed minimal hysteresis (as appeared in the inset of Fig. 6) which indicates the soft magnetic properties of the samples. The saturation magnetization (M_s), remanenent magnetization (M_r), magnetic moment (η_B) and coercive field (H_c) values of different compositions are given in Table 1.

The interactions between tetrahedral (A) and octahedral (B) sub-lattices in the spinel system (AB_2O_4) consist of inter-sub-lattice (A–B) super-exchange interactions and intra-sub-lattice (A–A) and (B–B) exchange interactions. Inter-sub-lattice super-exchange interactions of the cations on the (A–B) are much stronger than the (A–A) and (B–B) intra-sub-lattice exchange interactions [22]. The preferential occupancy of La^{3+} ions to the octahedral sites in the ferrite spinel will result in decreasing the concentration of Fe^{3+} ions in these sites, reduce the (B–B) exchange interactions and consequently reduce the (A–B) super-exchange interactions. In other meaning, the main contribution of magnetic properties derives from the highly magnetic Fe^{3+} ions (magnetic moment is fixed to be 5 μ_B (spin only)) present in the B sites. The successive replacement of Fe^{3+} ions by non-magnetic La^{3+} ions decreases the Fe^{3+}–Fe^{3+} (B–B) interactions. Since the magnetization per formula unit is represented by the net moment of that in A and B sites, thus, the slight decrease in the saturation magnetization with increasing La content can be attributed to the decreasing of the net magnetic moment as a result of magnetization dilution of the B-sublattice [23,24].

Furthermore, the deformity of the spinel lattice and increasing the nonlinear antiferromagnetic coupling between A and B sublattice due to La^{3+} substitution, decreases the saturation magnetization of samples [25]. Similar decrease in saturation magnetization of La^{3+} substituted Ni–Cu–Zn ferrite, synthesized through nitrate–citrate auto-combustion method, has been reported by Roy and Bera [8].

The coercivity represents the strength of the magnetic field that is necessary to surpass the anisotropy barrier and allow the magnetization of the nanoparticles following the magnetic field orientation. From Table 1 it can be observed that, all compositions exhibit low coercivity values, which is typical of soft ferrite with low magnetization to reverse spin direction [14]. Coercivity is a microstructure property. It depends upon defects, surface effect, strains, non-magnetic atoms, etc. in the material [8]. The coercive force variation of the system shows a typical size dependent behavior (Fig. 7). Similar results have also been reported earlier [26–28]. This behavior can be attributed to the combination of surface effect and its surface anisotropy [29]. The electronic configuration of La^{3+} ions results in the lattice or crystalline field distortion, and generates an internal stress. Also, the strong spin–orbit coupling of rare

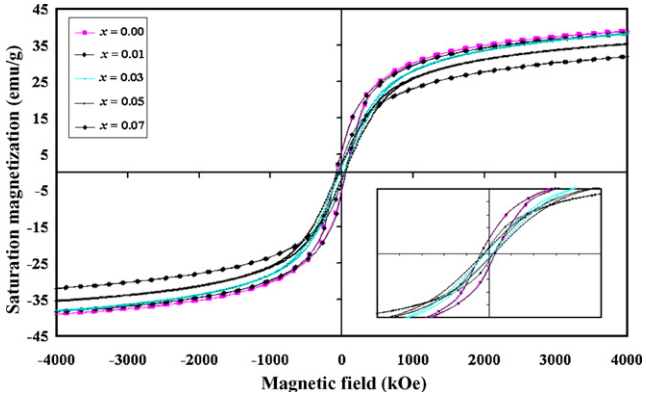

Fig. 6. Magnetic hysteresis loops for $Ni_{0.50}Cu_{0.25}Zn_{0.25}La_xFe_{2-x}O_4$ system calcined at 550 °C for 2 h.

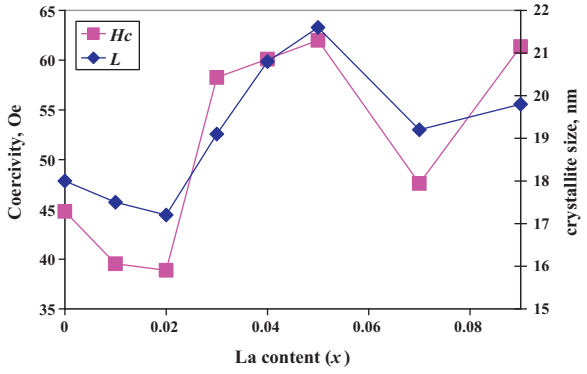

Fig. 7. Variation of the coercivity and crystallite size with La content in $Ni_{0.50}Cu_{0.25}Zn_{0.25}La_xFe_{2-x}O_4$ system.

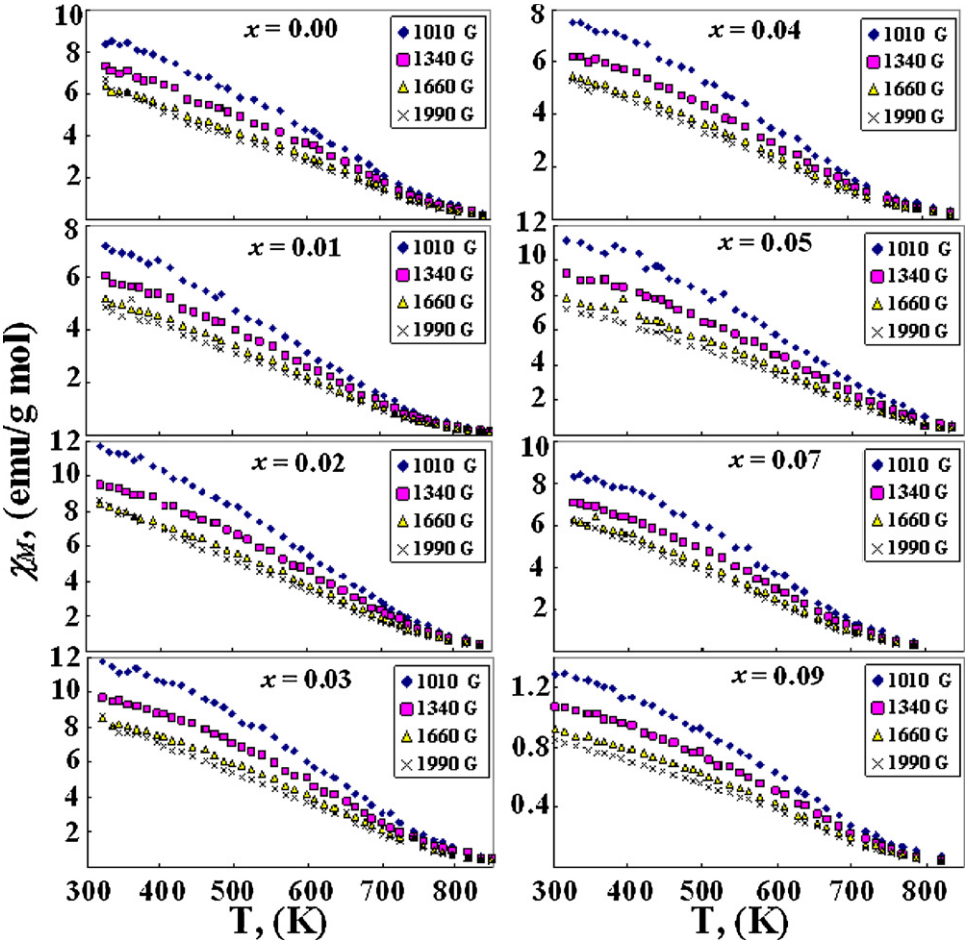

Fig. 8. Relation between molar magnetic susceptibility and absolute temperature as a function of different magnetic field intensities for $Ni_{0.50}Cu_{0.25}Zn_{0.25}La_xFe_{2-x}O_4$ system calcined at 550 °C for 2 h.

earth La^{3+} ions may contribute to the anisotropy, when they are located in the B sites of ferrite [30].

3.3.2. Susceptibility measurements

Fig. 8 correlates the variation of the molar magnetic susceptibility (χ_M) with absolute temperature as a function of the magnetic field intensity for the investigated ferrite samples. The same trend was obtained for all the investigated samples irrespective of their La content but with different values of both χ_M and the Curie temperature (T_C) (Table 1). The samples exhibit a ferromagnetic behavior in which the thermal energy is not quite sufficient to disturb the aligned moments of the spins. Near the transition temperature, the thermal energy is high enough to disturb all the aligned spins where χ_M decreases drastically, reaching the paramagnetic region after the transition temperature (T_C) at which a complete disordered state as well as the magnetization destruction is obtained. The large Curie temperature for these samples originates from the strong exchange interaction between the different sublattices [31].

From a closer look to Table 1, it is noticed that, the Curie temperature decreases with increasing La^{3+} ion content. This was expected since the La^{3+} ions of highly paramagnetic character decrease the ferromagnetic region at the expense of the paramagnetic one. As mentioned above, the octahedral occupancy preference of La^{3+} ions decreases the number of available iron and weakened the Fe^{3+}–Fe^{3+} interaction at octahedral sites. Also, the replacement of Fe^{3+} ions by higher ionic radius La^{3+} ions increases the un-symmetric structure of the samples, which increases the paramagnetic region and decreases the Curie temperature [32]. This observation may support the fact that La^{3+} ions replaces for Fe^{3+} ions in B sublattice of the investigated samples.

4. Conclusions

Single phase nano-crystalline La-substituted NiCuZn ferrites were successfully prepared using egg-white method. The incorporation of lanthanum was found to affect both the structural and magnetic properties. XRD showed single-phase cubic ferrite for all the investigated samples. The lattice parameters and XRD density were found to increase with increasing La content. FT-IR spectra assumed the octahedral preferentially occupancy of the lanthanum ions. Hysteresis loop measurements indicated a decrease in the measured saturation magnetization with increasing La content. Coercivity showed a size dependent behavior. The measured susceptibility exhibited

a decrease in the Curie temperature by the addition of lanthanum.

Acknowledgements

The authors are grateful to the Center of Research Excellence in Corrosion CoRE-C at King Fahad University for Petroleum and Mineral (KFUPM) for providing financial support for this work Via Grant No. CR-7-2010. Gabal acknowledges the facilities supported by King Abdul Aziz University in samples preparation. Also, the authors would like to express their thanks to Prof. Dr. M.A. Ahmed, Physics department, Faculty of Science, Cairo University, Egypt, for magnetic susceptibility measurements. Thanks are extended also to Dr. A. Awad for his help and cooperation.

References

[1] M.P. Reddy, W. Madhuri, M.V. Ramana, N.R. Reddy, K.V.S. Kumar, V.R.K. Murthy, K.S. Kumar, R.R. Reddy, J. Magn. Magn. Mater. 322 (2010) 2819.
[2] Z.H. Yang, Z.W. Li, L.B. Kong, J. Alloys Compd. 501 (2010) 173.
[3] H.I. Hsiang, W.C. Liao, Y.J. Wang, Y.F. Cheng, J. Eur. Ceram. Soc. 24 (2004) 2015.
[4] P.K. Roy, J. Bera, J. Magn. Magn. Mater. 321 (2009) 247.
[5] O.F. Caltum, L. Spinu, A.L. Stancu, L.D. Thung, W. Zhou, J. Magn. Magn. Mater. 160 (2002) 242.
[6] L. Zhao, H. Yang, L. Yu, Y. Cui, X. Zhao, S. Feng, J. Magn. Magn. Mater. 305 (2006) 91.
[7] S.E. Jacobo, S. Duhalde, H.R. Bertorello, J. Magn. Magn. Mater. 272–276 (2004) 2253.
[8] P.K. Roy, J. Bera, J. Magn. Magn. Mater. 320 (2008) 1128.
[9] J. Sun, J. Li, G. Sun, J. Magn. Magn. Mater. 250 (2002) 20.
[10] M.A. Ahmed, E. Ateia, L.M. Salah, A.A. El-Gamal, Mater. Chem. Phys. 92 (2005) 310.
[11] M.A. Ahmed, N. Okasha, M.M. El-Sayed, Ceram. Int. 33 (1) (2007) 49.
[12] E. Rezlescu, N. Rezlescu, P.D. Popa, J. Magn. Magn. Mater. 290–291 (2005) 1001.
[13] P.K. Roy, J. Bera, Mater. Res. Bull. 42 (2007) 77.
[14] M.A. Gabal, Mater. Res. Bull. 45 (2010) 589.
[15] M.A. Gabal, Mater. Lett. 64 (2010) 1887.
[16] T.K. Pathak, N.H. Vasoya, V.K. Lakhani, K.B. Modi, Ceram. Int. 36 (2010) 275.
[17] P. Kumar, S.K. Sharma, M. Knobel, M. Singh, J. Alloys Compd. 508 (2010) 115–118.
[18] N. Rezlescu, E. Rezlescu, C.L. Sava, F. Tudorache, P.D. Popa, Cryst. Res. Technol. 39 (2004) 548–557.
[19] R.D. Shanon, C.T. Prewitt, Acta Crystallogr. 1326 (1970) 1026.
[20] E. Manova, B. Kunev, D. Paneva, I. Mitov, L. Petrov, C. Estournès, C. D'Orléans, J.L. Rehspringer, M. Kurmoo, Chem. Mater. 16 (2004) 5689.
[21] R.D. Waldron, Phys. Rev. 99 (1955) 1727.
[22] M.G. Naseri, E.B. Saion, H.A. Ahangar, M. Hashim, A.H. Shaari, J. Magn. Magn. Mater. 323 (2011) 1745.
[23] M.L. Kahn, Z.J. Zhang, Appl. Phys. Lett. 78 (2001) 3651.
[24] J. Jiang, Y.M. Yang, L.C. Li, Physica B 399 (2007) 105.
[25] J. Jing, L. Liangchao, X. Feng, J. Rare Earths 25 (2007) 79.
[26] A.B. Gadkari, T.J. Shinde, P.N. Vasambekar, J. Magn. Magn. Mater. 322 (2010) 3823.
[27] M. George, S.S. Nair, A.M. John, P.A. Joy, M.R. Raman, J. Phys. D: Appl. Phys. 39 (2006) 900.
[28] J.F. Wang, C.B. Ponton, R. Grossinger, I.R. Harris, J. Alloys Compd. 369 (2004) 170.
[29] K. Maaz, A. Mumtaz, S.K. Hasanain, A. Ceylan, J. Magn. Magn. Mater. 308 (2007) 289.
[30] F.X. Cheng, J.T. Jia, Z.G. Xu, B. Zhou, C.S. Liao, C.H. Yan, J. Appl. Phys. 86 (2007) 2727.
[31] M.A. Ahmed, S.F. Mansour, S.I. El-Dek, Solid State Ionics 181 (2010) 1149.
[32] M.A. Ahmed, S.T. Bishay, J. Magn. Magn. Mater. 279 (2004) 178.